Middle East Journal of Agriculture Research
Volume: 12 | Issue: 04| Oct. – Dec. | 2023

EISSN: 2706-7955 ISSN: 2077-4605
DOI: 10.36632/mejar/2023.12.4.38
Journal homepage: www.curresweb.com
Pages: 587-608

Screening, Genetic Improvement, and Production Optimization of TA-Protease for Biofilm Removal of Dairy Sporeformers

Ahmad A. Radwan[1], Osama M. Darwesh[2], Karima A. Mohamed[1], Hala M. Abu Shady[3] and Maha T.H. Emam[1]

[1]Genetics and Cytology Dept., Biotechnology Research Institute, National Research Centre (NRC), Egypt.
[2]Agricultural Microbiology Dept., National Research Centre (NRC), Egypt.
[3]Microbiology Dept., Faculty of Science, Ain-Shams University, Egypt.

Received: 10 Sept. 2023 **Accepted:** 15 Oct. 2023 **Published:** 20 Oct. 2023

ABSTRACT

Spore-forming biofilms are the main pollutants found in the dairy industry. Although chemical and heat treatments are usually used to control these biofilms, they may become resistant; moreover, these treatments noticeably alter some milk properties, flavor, and taste as in food manufacturing. In this study, fourteen extracellular crude proteases were secreted by different thermo-alkali actinobacterial species and assessed as anti-biofilm biomolecules using a biofilm model of 10 mixed *Bacillus* species. Proteases produced by *Streptomyces sp.* ACD/G413 and *Streptomyces exfoliates* 15/G710 strains proved their fitness as anti-biofilm biomolecules; they exhibit biofilm removal percentages of 55% and 58.69% respectively. They were characterized as thermophilic alkaline proteases (TA-proteases) belonging to the serine type. Genetic improvement of proteases was achieved through EMS mutagenesis followed by interspecific protoplast fusion, which resulted in the construction of a new fusant named *St*-F.13 strain with an increase in the protease activity by 2.9-fold (395.89 U/ml) compared with that of the wild strain ACD/G413 (135.74 U/ml), which then potentially increased by 1.34-fold (533 U/ml) after applying statistical optimization by Plackett-Burman design and response surface methodology. Finally, these enzymes were effectively combined with biosynthesized ZnO_G240 nanoparticles to achieve 96.80% biofilm removal.

Keywords: Dairy biofilm eradication, TA-protease, Actinomyces, EMS mutation, Protoplast fusion.

1. Introduction

Biofilm-forming bacteria, which colonize the surfaces of dairy industry equipment, are the major problem affecting milk and its products' safety and quality. They cause spoilage of food products (Friedlander *et al*., 2019). Biofilm is formed by the accumulation of microbial cells joined by extracellular polymeric substances (EPS), thus negatively affecting the quality of the dairy industry (Bhosale *et al*., 2020). *Bacillus* spp. are the most prevalent genera that form biofilms in dairy manufacturing and are almost always harmful to dairy products (Angela *et al*., 2023).

The common method used in the dairy industry for biofilm removal is a cleaning-in-place (CIP) system. This method is not always effective due to some areas in production lines that are difficult to clean, such as joints, pipe corners, gaskets, etc., (Lequette *et al.,* 2010). Moreover, biofilms of spore formers are a daily challenge in the dairy industry, as the spores can survive not only pasteurization but also cleaning conditions **(**Cortés *et al*., 2011; Marchand *et al*., 2012). Thus, alternative or complementary approaches are required for achieving complete biofilm eradication. In recent times, degrading enzymes, such as proteases, have become a focus of interest as anti-biofilm cleaning agents due to their capability to degrade the major structural components of the biofilm matrix (Yang *et al*., 2023). Other studies reported that the addition of nanomaterials of certain metals exhibits significant anti-biofilm activity (Fulaz *et al*., 2019; Shkodenko *et al*., 2020; Mohd *et al*., 2020).

Corresponding Author: Maha T.H. Emam, Genetics and Cytology Dept., Biotechnology Research Institute, National Research Centre (NRC), Egypt. E-mail: maha_taimor@yahoo.com

The study objective is to combat the persistent biofilm problem in dairy industries using genetics tools and statistical optimization to improve protease enzyme production in combination with biosynthesized nanoparticles to provide an efficient approach alternative or complementary to the current clean-in-place (CIP) method for biofilm eradication in dairy industries.

2. Materials and Methods

2.1. The strains

Fourteen thermos-alkali protease-producing actinobacteria species were isolated from Egyptian harsh environments **(**El-Hawary, 2015, El-sherbiny *et al*., 2017; El-Hawary, 2018, Darwesh *et al*., 2019, Darwesh *et al.*, 2020), were screened for the ability to damage the biofilms formed in dairy industries. These species were provided by Dr. Ahmad S. El-Hawary, Faculty of Science, Al-Azhar University. Ten *Bacillus* strains, isolated in a previous study (Radwan *et al.,* 2022), were used in a mixed culture as a model of dairy biofilm.

2.2. Proteolytic index

The proteolytic actinobacteria were grown on ISP9 agar media supplemented with 1% casein and incubated at 55ºC for 48 hours. The proteolytic index was assessed by calculating the hydrolyzed zone diameter/colony diameter (Pratica *et al*., 2021).

2.3. Protease production

Production of protease enzyme was carried out by inoculating three discs (10 mm in diameter) cut from an actively growing agar culture of the desired strain into 100 mL of nutrient broth (NB) medium with a final pH of 8.5 and incubating overnight at 55ºC under shaking at 150 rpm. 40 mL of this culture were harvested, and the pellets were resuspended in 5 ml of phosphate-buffered saline (PBS). The suspensions were used to inoculate the complex medium for protease production (Darwesh *et al*., 2019) and incubated at 55ºC for 48 hrs. at 150 rpm. After incubation, the culture medium was centrifuged at 4000 rpm for 10 min at 4ºC, and the supernatant was recovered to be used as a crude enzyme source. Solubilized proteins in the culture supernatant were precipitated by acetone according to the method of Arulmani *et al*., (2007).

2.4. Protease activity assay

The protease activity assay was performed according to the method of Folin and Ciocalteau (1927). The crude enzyme was incubated with the casein substrate at a final concentration of 1% (w/v) in 50 mM Tris–Cl buffer (pH 8.5) for 10 min in a water bath at 55°C. After incubation, the reaction was terminated by the addition of 0.5 mL of 110 mM trichloroacetic acid (TCA) and incubated again for 30 min at room temperature (RT). The amino acids produced by the degradation of casein were measured by the Folin reagent and expressed as micromoles of tyrosine. A stock solution of standard L-tyrosine was prepared at 1.1 mmol (0.2 g per liter). The color development of the enzyme reaction and standard dilutions was measured at the optical density (OD) of 660 nm using a UV-VIS spectrophotometer (Model UV-240, Shimadzu, Japan). One unit of protease activity was defined as the amount of enzyme required to liberate 1 µmol of tyrosine per mL per minute under assay conditions.

2.5. Biofilm assays

2.5.1. Biofilm formation

The biofilm strains (10 *bacillus* sp.) were grown separately in NB medium at 37°C for 3-6 hrs. The obtained bacterial cells were collected and re-suspended in a sterile saline solution (0.85% NaCl). Then, the mixed suspension was used to inoculate 5 mL of 3% reconstituted skim milk (RSM) with a final concentration of 10^5–10^6 CFU and incubated at 37°C and 150 rpm for 72 hours, with the presence of sterilized stainless-steel surfaces of food-grade 316 (SS-316) (Radwan *et al*., 2022).

2.5.2. Biofilm eradication

Once incubation of biofilm strains with SS-316 coupons was completed, culture media was discarded, and coupons were rinsed three times with (1X) Phosphate-buffered saline (PBS) to remove the non-biofilm cells, transferred to a 15-mL falcon tube filled with 5 ml of enzymatic treatment (e.g., proteinase K or crude protease), and incubated for 30 min. Proteinase K (Bioline, Meridian Bioscience

Inc., USA) was used as a standard. Two controls were used, positive control of non-biofilm coupon and negative control of un-treated coupon. The enzymatic treatment was replaced by distilled water for both positive and negative control (Radwan *et al*., 2022).

2.5.3. Biofilm quantification by crystal violet (CV) assay

The evaluation of the formed biofilm was accomplished by CV assay (Sadiq *et al.,* 2017; Chen and Lee, 2018). Biofilm mass on the surfaces of coupons was first washed with PBS and fixed with methanol for 15 min. Then, coupons were transferred to 12-well plates, air-dried, and stained for 20 minutes with 1% CV solution. Afterward, the dyes were discarded, and coupons were rinsed five times with distilled water and air-dried again. Subsequently, coupons were immersed in 5 mL glacial acetic acid (33%) for 10–15 min to destain the stained biofilm with CV. Finally, biofilm quantity was detected by measuring the absorbance of the de-stained solution at 590 nm using a spectrophotometer (SHIMADZU, UV-240, Japan). Removal percentage was calculated by the formula [(control negative - test)/ control negative)] ×100.

2.6. Statistical analysis

One-way analysis of variance (ANOVA) was used to determine the significance through the Tukey test with a significance level (*p-value* <0.05).

2.7. Characterization of active anti-biofilm proteases

2.7.1. Determination of the proteolytic inhibitors

The extracellular crude enzymes of selected strains, ACD/G413 and 15/G710, were pre-incubated with inhibitors at concentrations of 2 mM for 15 min at 55 °C, and the residual proteolytic activities were determined under the standard assay conditions (Folin and Ciocalteau, 1927). The inhibitory effect was measured by comparing it with the control (without any inhibitor). Inhibitors used were β-mercaptoethanol, ethylene diamine tetraacetic acid (EDTA), iodoacetate (IAA), and phenyl methyl sulphonyl fluoride (PMSF) (Arulmani *et al.,* 2007).

2.7.2. Determination of optimal temperature and thermal stability

The optimal temperature of the selected proteases (ACD/G413 and 15/G710 strains) was determined by measuring the enzyme activity at various temperatures ranging from 30 to 90 °C in Tris-Cl buffer (pH 8.5) under the standard assay conditions (Folin and Ciocalteau, 1927). In addition, the thermal stability was measured by pre-incubating the enzymes at the same degrees of temperature for 30 min. Aliquots were taken to determine the residual enzyme activity under the standard assay conditions. The relative activity percentage was calculated by dividing the residual activity by the initial one and multiplying the value by one hundred (Mehdi *et al.,* 2018).

2.7.3. Determination of the pH activity and stability

The optimum pH of the proteolytic enzyme was determined at different pH values (pH 4–11) using 50 mM of the following buffers: citrate-phosphate (pH 4, 5, and 6); potassium phosphate (pH 7 and 8); tris-Hcl (pH 9); sodium carbonate-bicarbonate (pH 10), disodium phosphate-NaOH (pH 11). the enzyme assay was performed at the optimum temperature (70°C). For pH stability measurement, the enzymes were pre-incubated for 24 h in the previous pH buffers at RT. Then, the residual enzyme activity was measured. The relative activity percentage was calculated as mentioned above **(**Darwesh *et al.,* 2019)

2.8. Genetic improvement of anti-biofilm protease

2.8.1. Induction of EMS mutations

Ethyl methane-sulfonate (EMS) mutagenesis was carried out according to El-Sherbini and Khattab (2018). Spores of the selected strain (*St. exfoliates* 15/G710) were suspended in 5 ml of sodium phosphate buffer (100 mM, pH 7.0) and the EMS (Sigma-Aldrich Co, USA) was then added at a final concentration of 200 mM. The suspension was agitated at 100 rpm for 20, 40 and 60 min. The reaction was stopped by the addition of sodium thiosulfate (5%). Each treatment was washed and re-suspended in sodium phosphate buffer. Then, portions of 0.1 ml from suitable dilutions (10^{-1} to 10^{-5}) were spread on ISP9 medium supplemented with 1% casein and incubated at 55^{o}C for 48 hrs. Colonies developed

after incubation were counted and the survival percentages were estimated for each treatment. The selection was based on morphological changes and the zone of hydrolysis.

2.8.2. Protoplast fusion formation and regeneration

2.8.2.1. Protoplast formation

Firstly, for the determination of a marker for selection of protoplast fusants, antibiotic sensitivity tests were carried out on the superior mutant (15/G710_EMS.7) and the wild type *Streptomyces* sp. ACD/G413 using discs containing the following antibiotics with concentrations (µg/disc): ampicillin, 10; azithromycin, 15; chloramphenicol, 30; clindamycin, 2; gentamicin, 10; kanamycin, 30; rifampicin, 5; streptomycin, 10; tetracycline, 30; and vancomycin, 30. The responses were recorded and used as a selectable markers for fusant detection after protoplast fusion.

Then the methods of protoplast formation, fusion, and regeneration were performed according to Hopwood *et al*. (1985) and Okanishi *et al.,* (1974). Spores from fresh culture plates were inoculated in "S" medium and incubated at 55°C and 150 rpm. The culture after 48 h was transferred to fresh 'S' medium supplemented with 0.8% glycine and once again kept at 55°C in a rotary shaker until the middle of the exponential phase. The mycelia were harvested by centrifugation, washed with a solution of sucrose (0.3 M), and incubated in 'P' medium containing 10 mg of lysozyme/mL and 10 mg of bovine serum albumin (BSA)/mL (prepared prior to use by filter sterilization) at 37°C on a water bath shaker for 2 hrs. Protoplast formation was examined with a phase contrast microscope.

2.8.2.2. Protoplast fusion and regeneration

Protoplasts were collected by centrifugation at 2000 rpm for 10 min at 4°C. Then, the protoplast pellets of the parental strains were re-suspended in 0.1 mL 'P' medium and mixed with 0.9 mL of 40% (w/v) polyethylene glycol 400 (PEG 400) for two min. at RT, then the mixture were added to R2 soft agar medium and poured onto solidified R2 agar plates containing antibiotic mixture (30 µg/mL kanamycin and 5 µg/mL rifampicin). Plates were incubated for 7 days at 55ºC.

2.9. RAPD-PCR analysis

The extraction of bacterial DNA was performed by the lysozyme-sodium dodecyl sulphate method of Godson and Vapnek (1973), as described by Sambrook and Russell (2001). Random amplification of polymorphic DNA (RAPD) analysis was performed using four different primers Table (1). The amplified products were electrophoresed with one kb plus DNA ladder (Enzynomics, South Korea). Similarity matrix and dendrogram based on binary data of the banding patterns were constructed by NTSYSpc software version 2.10e.

Table 1: Primers used in (RAPD) analysis

No.	Name	Sequence (5'-3')	Annealing Temp.
1	RP1	GGGGTTTGCCACTGG	55 °C
2	RP2	CATACCCCCGCCGTT	
3	RP3	GTGTTGTGGTCCACT	
4	RP4	AACCTCCCCCTGACC	

2.10. SDS-PAGE and Zymogram assay

Protease crude extract was prepared as described above, and the protein content was quantified by the Lowry method (Lowry *et al.,* 1951). The sodium dodecyl sulfate-polyacrylamide gel electrophoresis (SDS-PAGE) was performed on a running gel containing 12% polyacrylamide by the method of (Laemmli, 1970). The zymogram was performed under a non-reducing condition using polyacrylamide gel, which contains casein (0.1%) as a co-polymerized substrate, as reported by Yasumitsu (2017). After electrophoresis, the protease activity was detected by the presence of a clear band against the blue background. The molecular weights of the bands were detected using the protein marker 245 kDa (cleaver scientific).

2.11. Optimization and stability of Protease production from *St*-F.13 fusant

The optimal conditions of protease production medium were screened and determined using MINITAB 18.1 (Minitab, Inc., PA, USA) for the experimental designs and subsequent analysis. In the Placket-Burman design, nine factors (independent variables) that might affect protease production were screened, at two levels (high and low) in 12 runs and one center point with three replicates. Based on the results obtained from Placket-Burman runs, a Central Composite design under response surface methodology was generated to determine the optimal levels of the selected variables for protease production by St-F.13. The Central Composite was comprised of 31 runs at five levels, varying the four significant parameters: glucose, peptone, casein, $CaCO_3$, and inoculum size. The data obtained were statistically analyzed, and the conditions for maximum production yield were predicted. A validation experiment was conducted in ten replicates to confirm the prediction.

Subsequently, the best fusant (*St*-F.13) was tested for its stability in protease production based on the proteolytic index level for six successive generations.

2.12. Visualization of the best treatments by CV stain and SEM imaging

The effect of crude protease of fusant St-F.13 alone and its combination with the synthesized ZnO_G240 nanoparticle were visualized by CV staining and scanning electron microscopy (SEM). For CV images, the biofilms after treatment were washed and stained as above without the final step of adding 33% acetic acid. For SEM images, the biofilms after treatment were washed with phosphate-buffered saline (PBS) and fixed with 2.5% glutaraldehyde in PBS at 4°C. After overnight incubation, the coupons were gently washed with PBS three times (10 min each), dehydrated in a gradient alcohol solution (25% for 30 min, 50% for 30 min, 75% for 30 min, 90% for 30 min, and 100% for 1 h), and placed into a desiccator for 3 days. The dehydrated coupons were then sputter-coated with gold and imagined under a scanning electron microscope (Zeiss Evo 10, Germany).

3. Results and Discussion

3.1. Assessment of protease as anti-biofilm bioagents

The extracellular crude proteases secreted by 14 thermo-alkali actinobacteria were assessed for removal of the dairy biofilms formed on food-grade stainless steel (SS-316) using mixed culture of ten *Bacillus* sp. The removal ability is illustrated in Fig. (1). The efficiency of the 14 proteases (50 mg/mL) in removing biofilms were compared to efficiency of the Proteinase K (Prot-K) with a concentration of (50 µg/mL) which has been reported to possess activity against a range of pathogens-forming biofilms (Kim *et al.*, 2013; Fleming and Rumbaugh, 2017; Raissa *et al.*, 2020; Liaqat *et al.*, 2021).

The obtained results from screening showed that, amongst the 14 proteases, a significant ($P<0.05$) removal was observed with crude enzymes of *Streptomyces* sp. ACD/G413 and *Streptomyces exfoliates* 15/G710, as lettered by "C" after ANOVA analysis with a Tukey test. The maximum removal was observed with the treatment of proteinase K, lettered by "D" as same as the non-biofilm-containing coupon (control +ve of removal). The removal percentages of Prot-K and crude of ACD/G413 and 15/G710 were 82.78%, 55 %, and, 58.69%, respectively. However, the results of biofilm removal for the remaining strains were not statistically significant. Consequently, the two strains, ACD/G413 and 15/G710, were chosen for more investigation.

Similar experiment was conducted by Park *et al.* (2012a) using culture supernatant of 458 actinomycete isolates to control the biofilm formation of *S. aureus*. They were identified 10 isolates, one belonged to genus *Kribbella* and nine belonged to *Streptomyces* genus, secrete antibiofilm protease demonstrate abilities more than 80%.

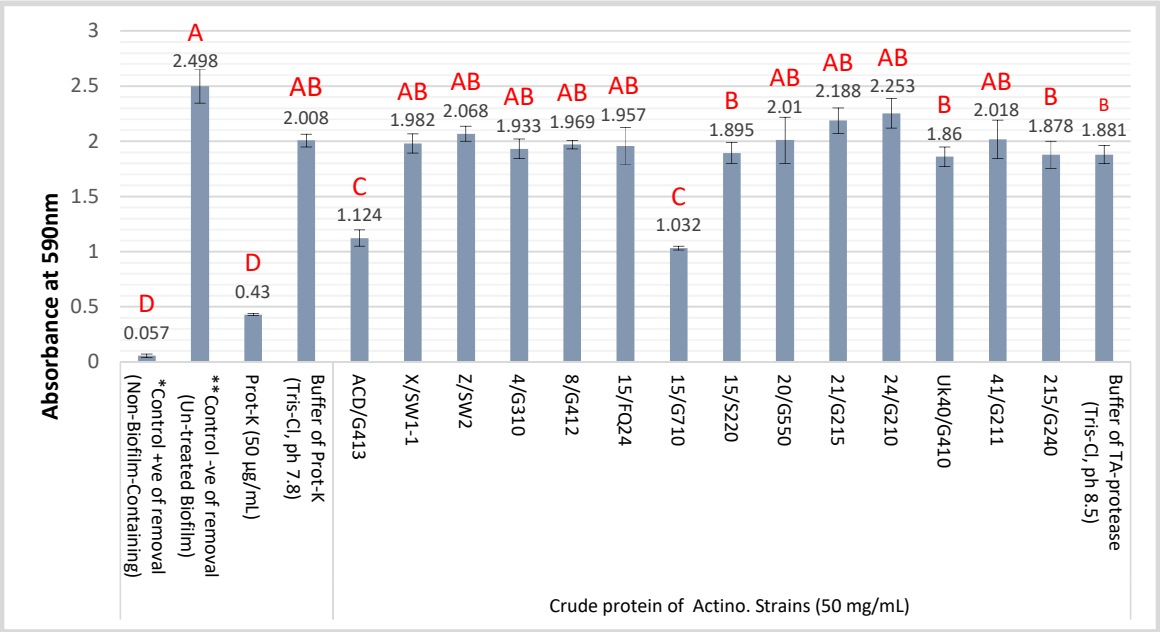

Fig. 1: Biofilm removal ability of 14 actinobacterial strains. Data represent means± standard error (SE) of three independent experiments. Values sharing the same letter are not significantly different at ($p < 0.05$) using Tukey test.

3.2. Characterization of selected proteases as anti-biofilm agents

3.2.1. Determination of the proteolytic inhibitors

The effect of protease inhibitors is explained in Fig. (2). The proteolytic activity of ACD/G413 and 15/G710 proteases were inhibited entirely in presence of PMSF, which is a well-known inhibitor of serine proteases (Khan *et al.*, 2011; Padmapriya *et al.*, 2012; Kamran *et al.*, 2015; Geng *et al.*, 2016; Lakshmi *et al.*, 2018; Fujii *et al.*, 2020; Sarkar and K., 2020). This finding suggesting that the secreted enzymes of ACD/G413 and 15/G710 could be categorized as a serine-type protease. A partial inhibition of 15/G710 protease in presence of EDTA was observed, these were reported earlier by various researchers (Yeoman and Edwards, 1994; Madan *et al.*, 2002; Khan *et al.*, 2011; Ibrahim *et al.*, 2015; Sarkar and K., 2020). On the other hand, the activity was slightly enhanced by the addition of β-mercaptoethanol. A similar observation has been previously documented about serine proteases (Ibrahim *et al.*, 2015; Kamran *et al.*, 2015). No effects were observed with IAA inhibitor. The results indicate that the secreted proteases of ACD/G413 and 15/G710 are serine-type. Many anti-biofilm proteases reported so far belong to the class of serine protease (Lequette *et al.*, 2010; Park *et al.*, 2012b; Park *et al.*, 2012a; Patil A, 2014; Meireles *et al.*, 2016; Mitrofanova *et al.*, 2017).

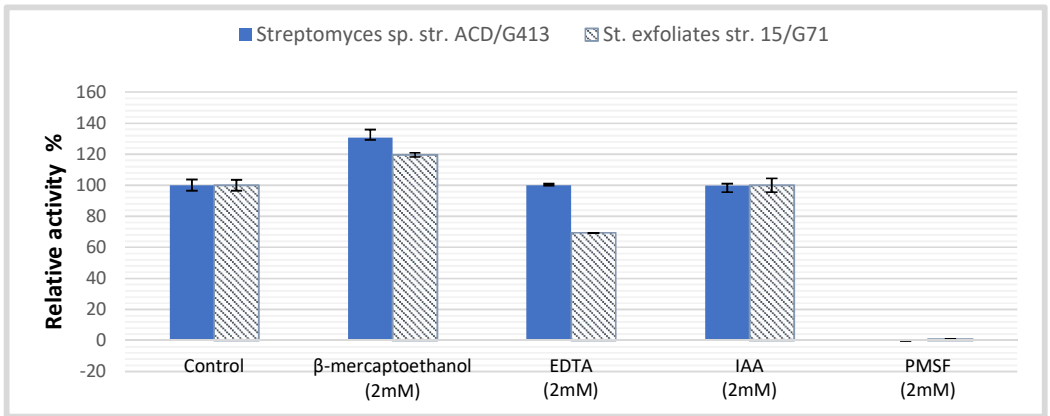

Fig. 2: Effect of enzyme inhibitors on the relative activity of proteases of ACD/G413 and 15/G710. The data are shown as means ± SE (n = 3).

3.2.2. Determination of optimum temperature and thermal stability

The effect of temperature on the enzymes activity and stability are summarized in Fig. (3). Activity of ACD/G413 and 15/G710 proteases were observed at a temperature range from 30 to 90°C and the highest activity was found at 70°C with protease activity 134.13 and 92.92 U/mL, respectively. Based on the optimum temperature, protease of ACD/G413 and 15/G710 could be classified as thermophilic proteases (Danson *et al.*, 1996). The structure of thermophilic enzymes is different when compared to the mesophilic ones. Thermophilic have a lot of salt-bridge structures and a greater number of main chain hydrogen bonds than mesophilic. Additionally, their protein structure has more hydrophobic amino acid residues than mesophilic proteins. This increases the enzyme activity at elevated temperatures (Afriani *et al.*, 2018; Sumardi *et al.*, 2018).

The thermal stability of two proteases was investigated by pre-incubation of the enzymes at different temperatures for 30 minutes. The stabilization profile revealed that the protease of 15/G710 was stable over a range 30-50°C more than ACD/G413, the residual was around 100 and 80%, respectively. However, activity of both after a further increase in temperature was decreased gradually as the temperature increase until reached zero. Previously it was reported that incubation of alkaline proteases at elevated temperatures promoting process of autolysis (self-digest) (Smolin *et al.*, 2020).

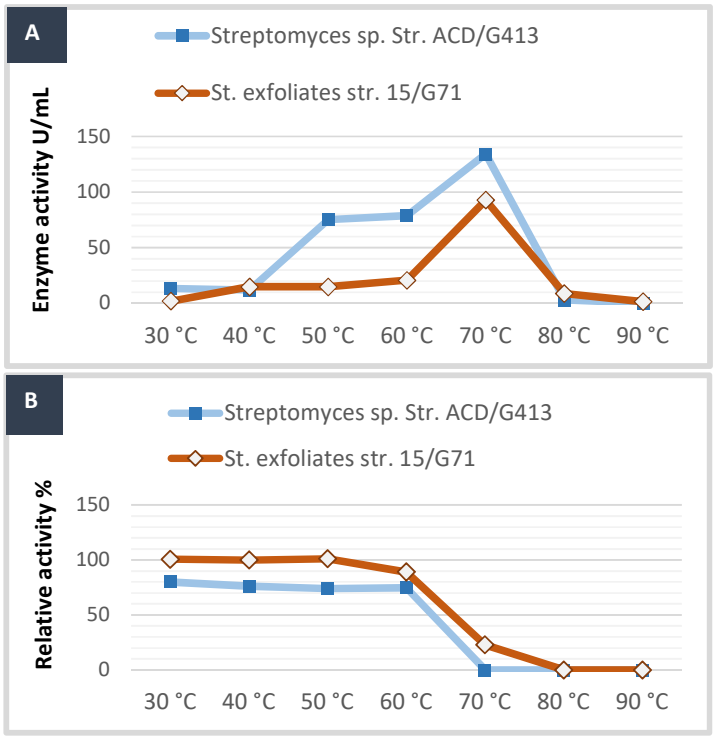

Fig. 3: Effect of temperature on enzyme activity and stability for ACD/G413 and 15/G710 proteases. **A)** Temperature effect on proteolytic activity represented as enzyme activity U/mL. **B)** Temperature effect on enzymes stability for 30 minutes represented as relative activity %. Each data point is the mean of three replicates.

3.2.3. Determination of the pH activity and stability

The influence of pH on activity and stability of selected proteases is showed in Fig. (4). Proteases of ACD/G413 and 15/G710 exhibited activity in a wide pH range and the maximum were found at pH 8.0 and pH 9.0, respectively. Alkaline proteases were mostly reported to have broad pH and the optima usually in the range of pH 8-12 (Madan *et al.*, 2002; Arulmani *et al.*, 2007; Khan *et al.*, 2011; Padmapriya *et al.*, 2012; Kamran *et al.*, 2015; Lakshmi *et al.*, 2018). Additionally, the two proteases were relatively stable in alkaline, maintained more than 70% of their relative activity at pH

range of 7-10. The enzymes activity and stability in alkaline condition, confirming that both are alkaline proteases.

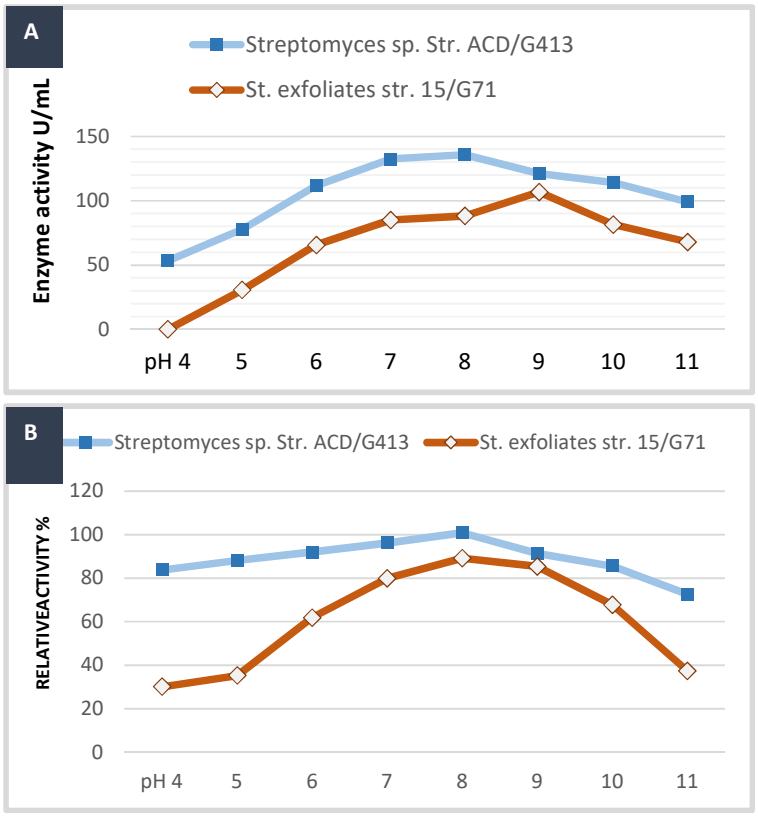

Fig. 4: Effect of pH on enzyme activity and stability for ACD/G413 and 15/G710 proteases. **A)** Effect of pH on proteolytic activity represented as enzyme activity U/ml. **B)** Effect of pH on enzymes stability for 24 h represented as relative activity %. Each data point is the mean of three replicates.

3.3. Genetic improvement of TA-protease strains

3.3.1. Induction of EMS mutations

The strain *St. exfoliates* 15/G710 was subjected to mutagenic treatment by EMS, one of the well-known chemical mutagenic agent that induce G/C to A/T transitions randomly (Freese, 1961). Figure (5) shows the survival percentage of EMS treatment and protease productivity of nineteen randomly selected mutants out of the survived isolates. As expected according to that reported previously (El-Sherbini and Khattab, 2018; El-sayed *et al.*, 2019), the surviving ratio was decreased as the time of treatment increased because of the lethal effect of EMS. The lowest survival (0.81%) was recorded at the time of sixty minutes.

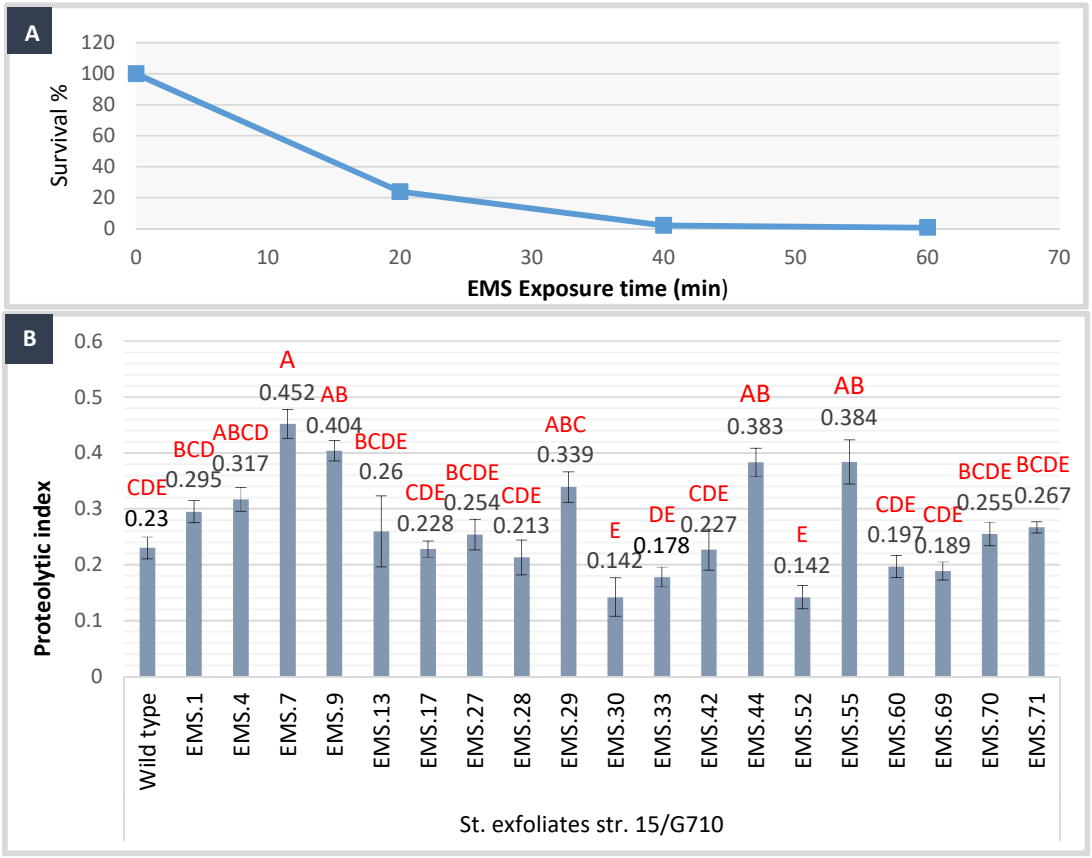

Fig. 5: Analysis of EMS mutation of *St. exfoliates* 15/G710. **A)** The survival percentage of EMS treatment. **B)** The protease productivity of 19 randomly selected mutants represented as a proteolytic index. Each data present is the mean of three replicates. Values sharing the same letter are not significantly different at ($p < 0.05$) using Tukey test.

Analysis of protease productivity of selected EMS mutants statistically showed a significant ($P<0.05$) difference in proteolytic index of mutant EMS.7, as lettered by "A" after ANOVA with a Tukey test. This mutant recorded the highest proteolytic activity by 1.96-fold when compared to the wild type. The nearest productivity was recorded by mutants EMS.9, EMS.44, and EMS.55, as lettered by "AB". They proved to have productivity more than wild type and a little bit less than EMS. Meanwhile, there three selected mutants (EMS.33, EMS.30, and EMS.52) their calculated proteolytic index were less than the significant level of the wild type. In general, it could be concluded that EMS mutagenic treatments improved TA-protease production of *St. exfoliates* 15/G710 strain. Similar finding was reported on other *Streptomyces* strains (Bhavani *et al.*, 2012).

3.3.2. Protoplast fusion

Protoplast fusion is a very useful technique for strains improvement by exchanging the genetic material between two cell types to obtain fusant with desired properties (Verma *et al.*, 2008). In this study, interspecific protoplast fusion was conducted between two *Streptomyces* species, the superior mutant of EMS treatment *St. exfoliates* 15/G710_EMS.7 and the wild strain *Streptomyces* sp. ACD/G413, to obtain fusant(s) with higher TA-protease production than the parental strains.

First, antibiotic-resistance pattern of parent strains toward 10 different antibiotics was examined to determine the possible selective marker for detection and isolation of their fusant(s), see Table (2). As shown, the strain15/G710_EMS.7 was resistant to ampicillin, clindamycin, and kanamycin and sensitive to the others tested. Meanwhile, strain ACD/G413 was resistant to ampicillin, azithromycin, clindamycin, and rifampicin and sensitive to the others. From these antibiotics' responses, we can use kanamycin and azithromycin or rifampicin as a selectable marker in protoplast fusion experiment.

Table 2: Antibiotic-resistant patterns of parent strains of protoplast fusion.

No.	Antibiotics	Zone diameter (mm)	
		15/G710_EMS.7(Mutant)	ACD/G413 (Wild type)
1	**Ampicillin** (AM, 10µg)	-	-
2	**Azithromycin** (AZ, 15µg)	8	-
3	**Chloramphenicol** (C, 30µg)	13	15
4	**Clindamycin** (DA, 2µg)	-	-
5	**Gentamicin** (CN, 10µg)	13	42
6	**Kanamycin** (K, 30µg)	-	20
7	**Rifampicin** (R, 5µg)	22	-
8	**Streptomycin** (S, 10µg)	30	44
9	**Tetracycline** (TE, 30 µg)	30	8
10	**Vancomycin** (VA, 30 µg)	18	28

Protoplast was obtained by lysozyme treatment and samples were taken periodically under phase contrast microscope to examine protoplast formation Fig. (6). After fusion, all grown colonies (15 fusants) on regeneration media containing the selective marker kanamycin and rifampicin were picked on ISP9/casein plates for estimating the protease productivity of fusants by measuring their hydrolytic zone. The enzyme productivity of fusants is summarized in Fig. (7). The fusants were coded here by symbol *St* for referring to their parental strains which were two *Streptomyces* species, symbol F for fusant, and numbers from 1 to 15.

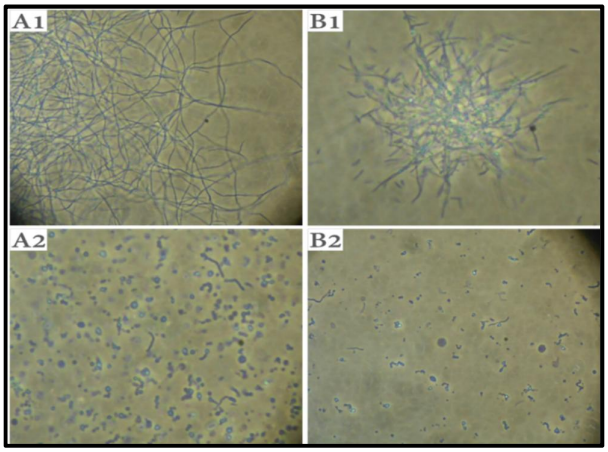

Fig. 6: Microphotograph for protoplast formation **A1, B1)** Strain 15/G710_EMS.7 and ACD/G413, respectively, before protoplasting. **A2, B2)** Strain 15/G710_EMS.7 and ACD/G413, respectively, after protoplasting.

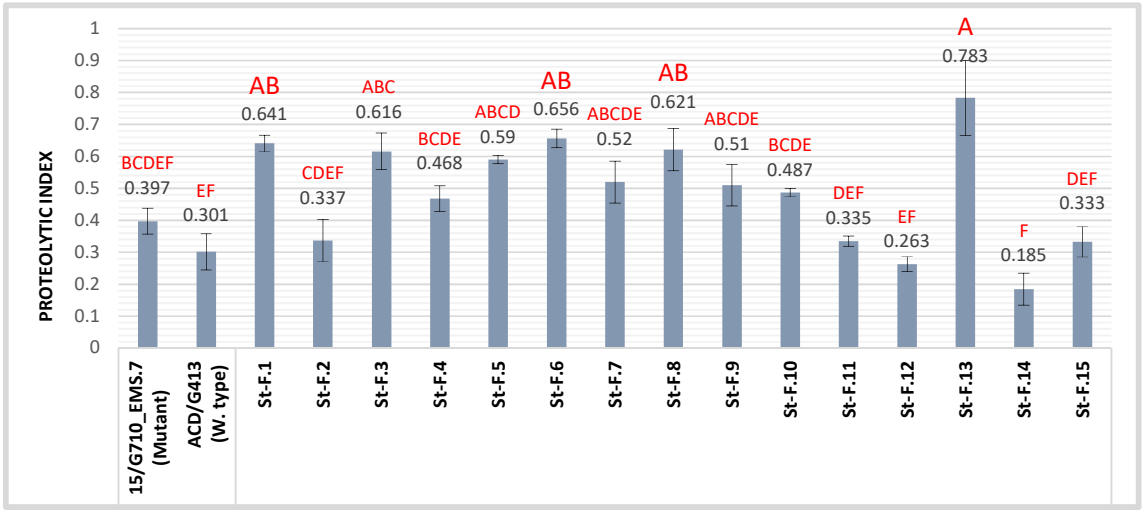

Fig. 7: Proteolytic index of protoplast fusion of *St. exfoliates* 15/G710_EMS.7 and *Streptomyces* sp. ACD/G413. Data represent means± SE. Values sharing the same letter are not significantly different at ($p < 0.05$) using Tukey test.

The results shown a significant (P<0.05) proteolytic activity expressed by fusant *St*-F.13, as lettered by "A" after ANOVA with a Tukey test. This fusant exhibited the highest activity by 1.97-fold when compared to the highest parent (strain 15/G710_EMS.7). In contrast, the proteolytic activity of other fusant did not differ significantly when compared to the parents. This result usually obtain in protoplast fusion when partial or incomplete genetic recombination have been done (Prabavathy *et al.*, 2006).

Subsequently, the best fusant (*St*-F.13) was tested for its stability in protease production for six successive generations, Fig. (8). As observed, the selected fusant was stable at its proteolytic index level over studied period (6 generations). Additionally, this fusant was further assessed for protease production in submerged culture. Figure (9) shows protease activity of fusant *St*-F.13, parental strains 15/G710_EMS.7 (mutant) and ACD/G413 (Wild type), and strain 15/G710 (Wild type). The obtained data confirm over productivity of fusant *St*-F.13 than its parental strains, by 2.9-fold increases than the highest wild type ACD/G413. The protease activity of *St*-F.13 was 395.89 U/mL, while of parent strains 15/G710_EMS.7 and ACD/G413 were 202.2 and 135.74 U/mL.

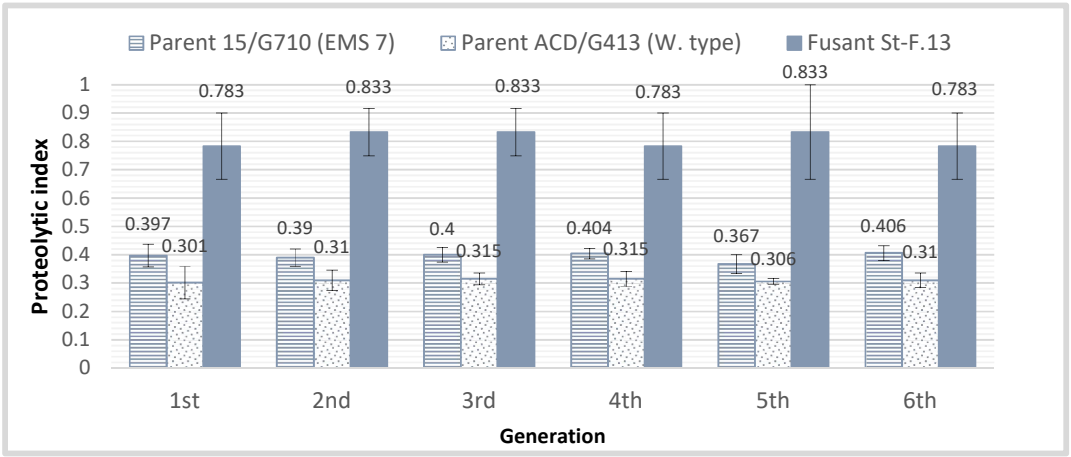

Fig. 8: Protease production stability of fusant *St*-F.13 for six generations, represented as a proteolytic index. The data are shown as means ± SE (n = 3).

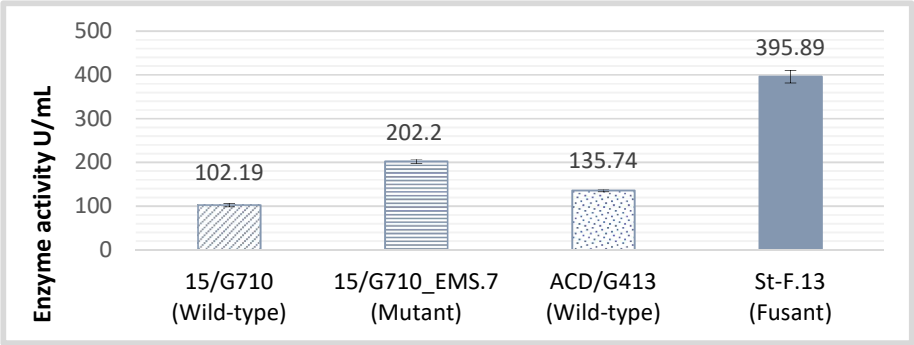

Fig. 9: Protease activity of fusant *St*-F.13 and its parents. One unit of protease activity was defined as the amount of enzyme producing 1.0 µmol of tyrosine per min/ml. The data are shown as means ± SE (n = 3).

Khattab and Abdel-Aziz (2012) improved alkaline protease production of *Streptomyces* sp. from 223.08 to 715.99 U/mL using UV-irradiation followed by protoplast fusion. Bazaraa *et al.* (2021), induced EMS mutagenesis followed by intergeneric protoplast fusion between two lactic acid bacterial strains to enhance bacteriocins production. Interspecific *Streptomyces* protoplast fusion has been previously reported by Zhou and Zhou (1989), Qi and Zheng, (1990), and El-fadly *et al.* (2009) for improvement antibiotic production. Therefore, this study considers to be the first report of interspecific protoplast fusion between two *Streptomyces* strains for purpose of TA-protease production improvement as well as application of EMS mutagenesis before protoplasting. In general, less attention have been paid to Actinomycetes proteases comparing to others bacterial proteases, particularly which produced by *Bacillus* (Mehtani *et al.*, 2017).

3.4. Molecular analysis of fusant (*St*-F.13)

3.4.1. RAPD-PCR analysis

The molecular method of random amplification of polymorphic DNA (RAPD) was used to study the genetic relationship among the fusant strain (*St*-F.13) and the parent strains (15/G710_EMS.7 and ACD/G413). The RAPD analysis was detecting a total of 31 different bands produced by four 15-mer primers, 6 bands were found to be monomorphic and 25 bands were polymorphic Fig. (10). Similarity matrix and dendrogram based on RAPD analysis illustrated in Fig. (11).

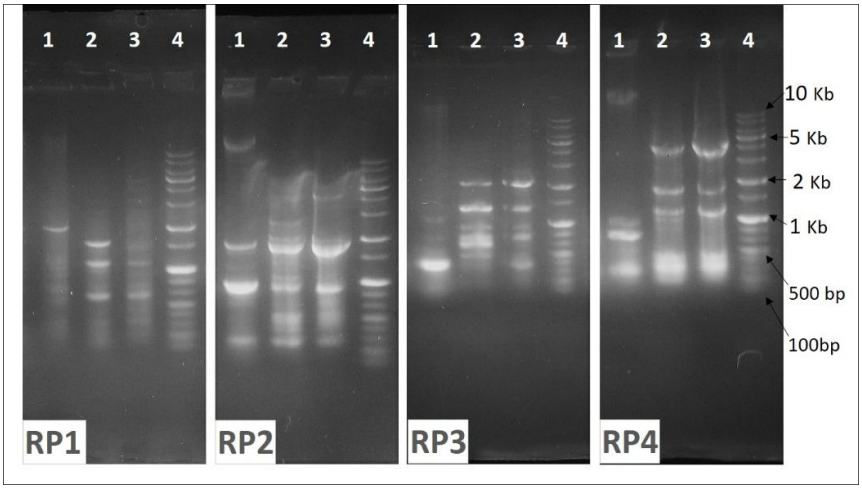

Fig. 10: Gel electrophoresis of RAPD analysis. Lane: 1. parental strain 15/G710_EMS.7; 2. parental strain ACD/G413; 3. fusant *St*-F.13; 4. One kb Plus DNA Ladder (Enzynomics, South Korea).

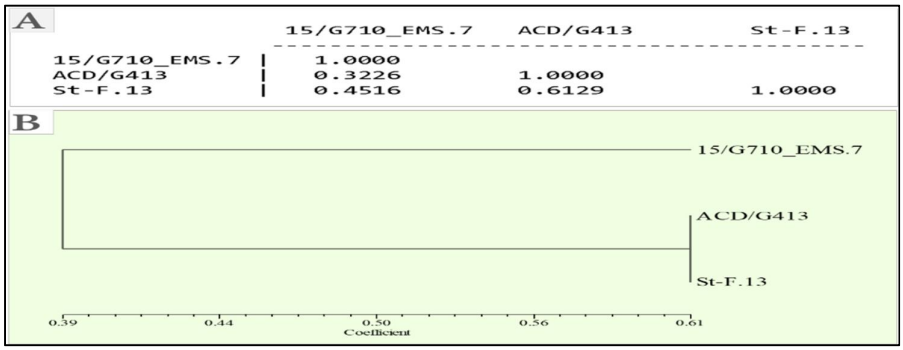

Fig. 11: Similarity matrix (**A**) and Dendrogram (**B**) based on RAPD banding patterns of fusant *St*-F.13 and parental strains 15/G710_EMS.7 and ACD/G413.

3.4.2. SDS-PAGE and Zymogram assay

The extracellular crude enzymes of fusant *St*-F.13 and its parents 15/G710_EMS.7 and ACD/G413 was analyzed by SDS-PAGE and Zymogram assay Fig. (12). As shown in SDS-PAGE pattern, there is a genetic variations between the fusant *St*-F.13 and its parental strains, it is observed, the presences of one unique band in *St*-F.13 different from its parent, indicating the recombination of parental genome in the fusant (Zhang *et al.*, 2009; Lu *et al.*, 2013). Furthermore, a genetic similarity between fusant *St*-F.13 and its parent was observed. This results was in agreement with Chakraborty and Sikdar (2008) and Lu *et al.* (2013), who reported that the fusant had an unbalanced inheritance of genetic material from its parental strains.

Also, zymogram assay was performed to determine the molecular weights of secreted proteases of fusant *St*-F.13 and its parents, the results showed a clear hydrolytic zone of proteolytic activity in zymogram lanes of fusant and its parents with a molecular mass of approximately 48 kDa. An alkaline serine protease 48 kDa produced by *Bacillus subtilis* D9 was reported by Mahmoud *et al.* (2021). Mechri *et al.* (2017) characterized a thermophilic alkaline protease (51 kDa), and Maeda *et al.* (2011) reported also a serine-type protease (40-kDa).

Moreover, zymogram of strain 15/G710_EMS.7 showed presence of another two extracellular enzymes with molecular masses of approximately 250 and 100 kDa. We suggested that, those appeared zones might be produced by other types of proteases inherited from its wild type or by either glycosylated or aggregated proteases as they were at high molecular masses (Dalmaso *et al.*, 2015).

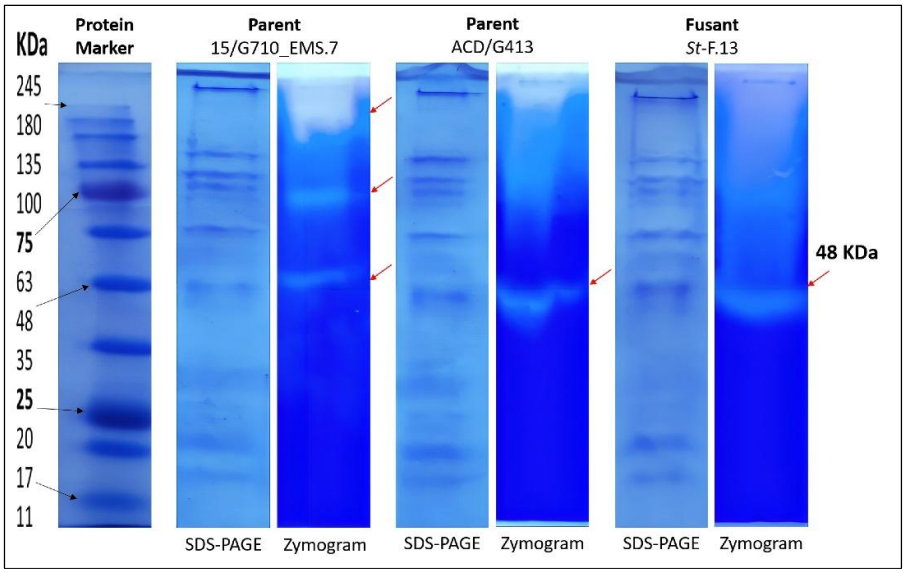

Fig. 12: SDS-PAGE and Zymogram analyses for fusant *St*-F.13 and parental strains 15/G710_EMS.7 and ACD/G413. The protein marker 245 kDa (cleaver scientific).

3.5. Production optimization of fusant *St*-F.13 protease

3.5.1. Plackett-Burman design

The influence of nine independent variables (shaking speed, temperature, time, pH, casein, glucose, peptone, $CaCO_3$, and inoculum size) on protease production of fusant (*St*-F13) was detected using the Plackett-Burman design. Protease activity (U/mL) was chosen also in this study as the yield for statistical optimization. The Pareto chart and main effect plots of the current Plackett-Burmann are showed in Fig. (13), generated in MINITAB.

Interestingly, the Plackett-Burman design revealed that the peptone (digest of casein) is the best carbon source for increasing the protease productivity, neither casein nor glucose. Moreover, the incubation time isn't a significant factor although it showed a positive effect on the productivity in the main effect plots. According to the Plackett-Burman, the four most significant factors identified in the Pareto chart ($P<0.05$), i.e., glucose, peptone, $CaCO_3$, and inoculum size were selected for further optimization by a response surface methodology with Central Composite design. Though glucose had a negative effect as shown in main effect plots, it was selected to find out the exact amount at which the fusant strain could produce maximum protease activity. The other factors tested with Plackett-Burmann were included in all runs at one level, either minimum or maximum, according to its effect on the production as explained in main effect plots.

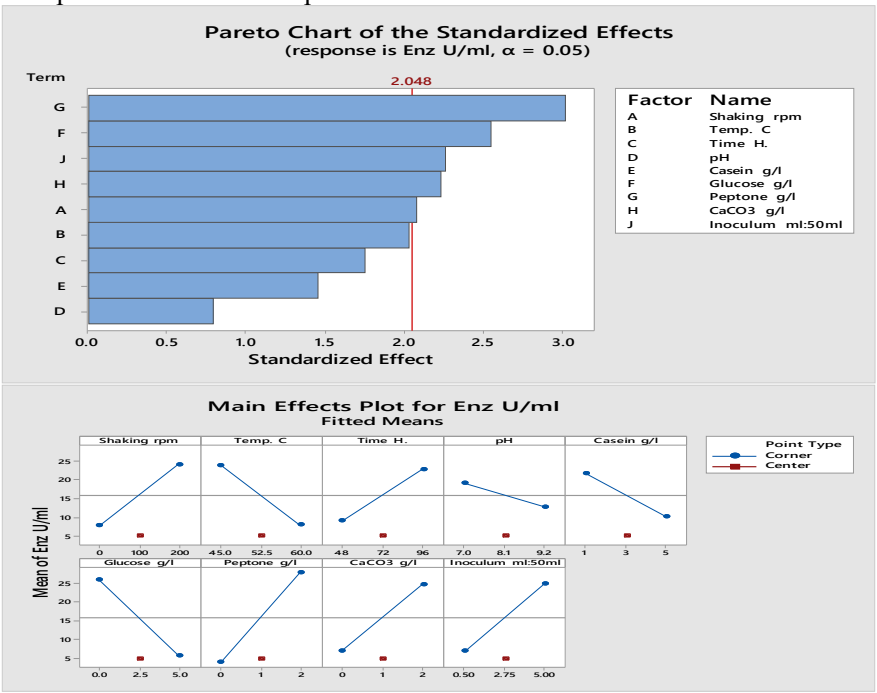

Fig. 13: Pareto chart and main effect plots of Plackett–Burman design for production optimization of *St*-F13 protease. Pareto chart showing the significant parameters affecting the production. Main effect plots showing the effect of nine screened factors on protease production.

3.5.2. Central Composite design

The model was statistically analyzed, and ANOVA of the regression model demonstrate that it is significant ($P<0.05$) and acceptable for optimizing protease conditions. The predicted maximum protease activity was 505.13 U/mL, and the optimum levels of selected factors were calculated as glucose 0.25 g/L, peptone 5.0 g/L, $CaCO_3$ 5.0g/L, and inoculum size 8.5 ml/50ml Fig. (14). In comparison to the reaction optimization conditions, the recommended levels of temperature and pH have been reduced to their minimum levels to increase the enzyme productivity.

The validation model was carried out using a t-test at the 5% level Table (3), there was no significant difference between the observed and predicted protease activity (t-test; $P > 0.05$). As a result, the model was accepted and the same conditions were applied for the production of the final protease. The protease productivity of fusant *St*-F13 under optimized conditions was increased to 1.34-fold (533 U/ml) when compared to the initial conditions (395.89 U/ml). Kumar and co-workers reported 1.32 fold

increase in protease production after optimization by Plackett–Burman design and response surface methodology (Kumar *et al.*, 2018). Ramkumar *et al.*, (2018) found that the production of alkaline protease of *B. licheniformis* NK increased to 1.5-fold by optimization of the cultivation medium. A study reported by Sharma *et al.* (2021) showed that alkaline protease production by *B. amyloliquefaciens* SP1 was increased to 2.1 fold after optimization. A more than four folds increase in protease production after optimization using Plackett–Burman design and response surface methodology was reported by Mechri *et al.* (2017) and David *et al.* (2018).

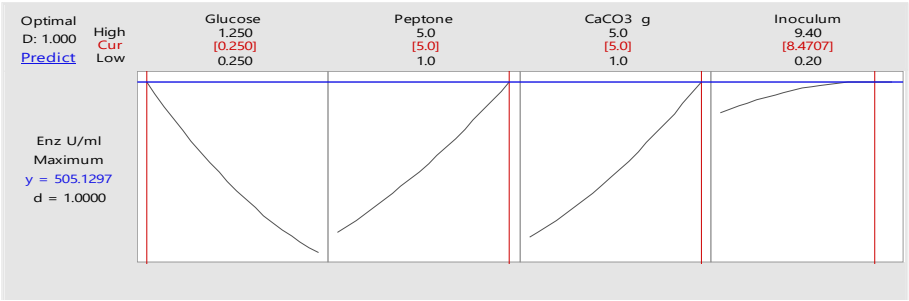

Fig. 14: Optimization plot of Central Composite design for production optimization of *St*-F13 protease.

Table 3: Validation experiment for optimization model of Central Composite design

	Absorbance (660nm)	Tyrosine (µmol)	Enzyme activity (U/mL)	Mean	Std. Error	T-Value	P-Value
1	1.8654	916.65	498.6229	533	11.2	2.48	0.035
2	1.8366	901.31	485.441				
3	2.0458	1012.74	544.4516				
4	1.9104	940.74	508.8589				
5	1.8653	916.65	493.718				
6	2.0658	1063.44	569.8682				
7	2.1012	1086.32	587.6134				
8	1.9816	978.86	533.232				
9	2.0527	1032.93	568.1115				
10	1.9932	985.07	539.8443				

3.6. Combination effect of fusant *St*-F.13 with green nanoparticles for biofilm eradication

The effect of crude protease of fusant *St*-F.13 alone and in combination with the biosynthesized metal/metal oxide nanoparticles, which synthesized in a previous study (Radwan *et al.*, 2022), were evaluated on the above-mentioned model of dairy biofilm. Accordingly, concentration of 50 µg/mL was suggested for NPs treatment. However, concentration of 50 mg/mL was used for crude enzyme. The results in Table (4) showed significant removal effect of biofilm by crude protease of *St*-F.13 in combination of the synthesized ZnO_G240 NPs, 96.80%, comparing with the *St*-F.13 protease alone, 71.23%. The CuO_G240 NPs exhibited less removal activity than ZnO_G240 with the same combination treatment recording 88.64%. The Toxicity evaluation of ZnO_G240 NPs by brine shrimp bioassay was done in a previous study (Radwan *et al*., 2022), and the results showed that, The ZnO_G240 NPs at the active concentration for biofilm eradication are safe and do not have toxicity.

Table 4: Combination effects of crude protease of St-F.13 with green synthesized NPs on biofilm removal.

		Absorbance (590nm)			Mean	Std. Error	Removal (%)
+ve control removal (Non-Biofilm-Containing)		0.066	0.042	0.061	0.0563	0.00731	97.68
-ve control removal (Un-treated Biofilm)		2.559	2.448	2.283	2.43	0.0802	0
Crude protease of *St*-F.13 (50 mg/mL)		0.625	0.718	0.754	0.699	0.0384	71.23
Crude protease of *St*-F.13 (50 mg/mL) + Green synthesized NPs (50 µg/mL)	Ag_G310	0.688	0.738	0.741	0.722	0.0172	70.28
	Ag_G210	0.655	0.733	0.645	0.678	0.0278	72.10
	Ag_G240	0.681	0.706	0.704	0.697	0.00802	71.31
	CuO_G215	0.706	0.698	0.688	0.697	0.00521	71.31
	CuO_G210	0.746	0.689	0.733	0.723	0.0172	70.24
	CuO_G240	0.291	0.272	0.264	0.276	0.00801	88.64
	ZnO_G412	0.703	0.663	0.743	0.703	0.0231	71.07
	ZnO_G710	0.71	0.745	0.687	0.714	0.0169	70.61
	ZnO_G215	0.648	0.703	0.711	0.687	0.0198	71.73
	ZnO_G240	0.048	0.086	0.099	0.0777	0.0153	96.80

Removal percentage based on the mean absorbance of three replicates was calculated by the formula [(control negative - test)/ control negative)] ×100.

3.7. Visualization of the biofilm removal treatments by CV stain and SEM imaging

The effect of fusant *St*-F.13 crude protease on the performed biofilm, as well as when combined with the biosynthesized ZnO_G240 NPs have been clearly demonstrated by CV stain and SEM (scanning electron microscopy), Fig. (15).

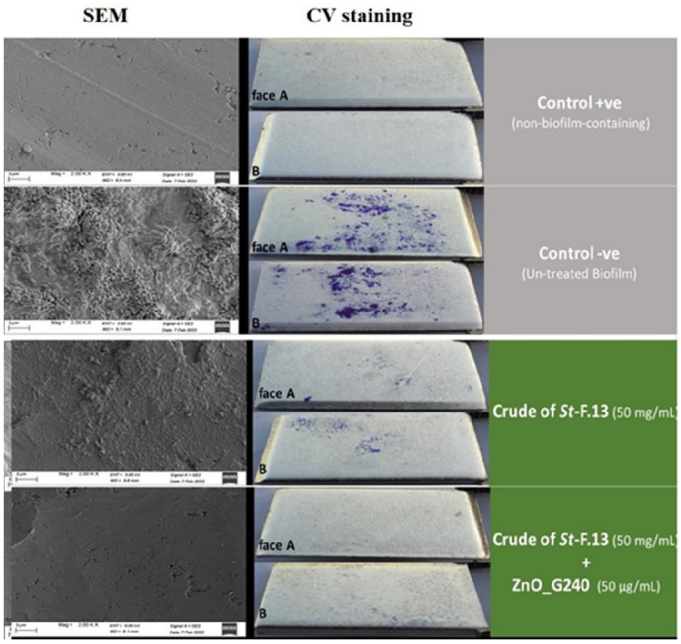

Fig. 15: Visualization of the best treatments for dairy biofilm eradication on food-grade stainless steel (SS-316) by crystal violet stain and SEM imaging.

Images of SEM at 2,000×, were consistent with the CV stain images, showed that the combination of the ZnO_G240 NPs with *St*-F.13 crude protease caused complete removal for attached biofilms on stainless steel surface. The images confirmed the synergistic interaction between the NPs

ZnO_G240 and *St*-F.13 protease. Moreover, the images revealed that the treatment with *St*-F.13 protease alone has great degradation, decreased the biofilm layers as well as reduced the number of cells attached to stainless steel surface with more extended areas of complete dispersal when compared to untreated coupon (control -ve). Also, it was observed the coupon of *St*-F.13 protease treatment is covered with milk protein layer that have been described as the important factor aiding the initial cells adherence onto surfaces (Sadiq *et al.*, 2017; Shemesh and Ostrov, 2020), but these were disappeared after combination treatments with NPs ZnO_G240.

Further study on *St*-F.13 protease and its mechanism of biofilms degradation is needed, but we can conclude the mechanism of *St*-F.13 protease in biofilm removal from the previously studied proteinase K (Prot-K) which has frequently been used as efficient biofilm removal agent (Fleming and Rumbaugh, 2017; Jee *et al.*, 2020; Liaqat *et al.*, 2021). The known mechanism of biofilm dispersion by Prot-K, is cleaving the peptide bonds of aliphatic, aromatic, or hydrophobic amino acids in the EPS matrix which leads to degradation of the protein components and disintegration of the established biofilms (Chaignon *et al.*, 2007; Liaqat *et al.*, 2021).

In the other hand, the key mechanism by which ZnO NPs work to destroy the bacterial biofilm is the formation of reactive oxygen species (ROS), the synthesized ZnO NPs inhibits the respiratory enzyme(s) therefore, the generation of ROS is facilitate, the formed ROS can irreversibly damage the bacteria membrane, DNA, mitochondria, etc. (Dwivedi *et al.*, 2014; Abdelghafar *et al.*, 2022). From that, we can infer a mechanism of synergism between crude protease and NPs ZnO_G240. After the initial treatment with crude protease, the associated proteins in the EPS matrix were extensively degraded and the biofilm cells became loose. This enables the ZnO NPs to deeply penetrate the biofilm and completely eradicate the existing cells.

4. Conclusion

The protease is the most potent enzyme in biofilm dispersion. In this study, proteases from two actinomyces species were subjected to genetic improvement using EMS mutation followed by protoplast fusion and optimization conditions for production of crude protease to increase the biofilm removal efficiency in dairy industry. The biofilm removal percentage of selected wild type strains ACD/G413 and 15/G710 were 55 %, and, 58.69%, respectively. After applied genetic improvement and optimization of protease production, the biofilm removal percentage increased to 71.23% by fusant strain (*St*-F.13). Moreover, when the *St*-F.13 protease combined with the green synthesized ZnO_G240 NPs, the biofilm removal percent reached 96.80% which is more than the standard commercial Proteinase K (82.79%).

The results from the current study offers new potential cleaning agent for application in dairy industries composed of biosynthesized NPs (ZnO_G240) and (*St*-F.13 proteases), after more investigation might be produced industrially cheaper.

Abbreviations

ANOVA: Analysis of variance; BSA: Bovine Serum Albumin; CIP: Clean-In-Place; CV: Crystal Violet; EDTA: Ethylenediaminetetraacetic acid; EMS: Ethyl methane-sulfonate; EPS: extracellular polymeric substances; IAA: Iodoacetate; NPs: Nanoparticles; PBS: Phosphate Buffered Saline; PEG: Poly ethylene glycol; PMSF: Phenyl Methyl Sulphonyl Fluoride; RAPD: Random amplification of polymorphic DNA; ROS: reactive oxygen species; RSM: Reconstituted Skim Milk; SDS-PAGE: Sodium Dodecyl Sulfate-Poly acrylamide gel electrophoresis; SEM: Scanning Electron Microscopy; SS-316: Stainless Steel food-grade (316) ; TA-protease: Thermophilic Alkaline Protease; TCA: Trichloroacetic acid.

Acknowledgements

The authors gratefully acknowledge Dr. Ahmad S. El-Hawary, Faculty of Science, Al-Azhar University for providing us with actinomycetes strains.

Fund

This research was funded by the National Research Centre (NRC), Egypt.

References

Abdelghafar, A., N. Yousef, and M. Askoura, 2022. Zinc oxide nanoparticles reduce biofilm formation, synergize antibiotics action and attenuate *Staphylococcus aureus* virulence in host; an important message to clinicians. BMC Microbiol. 22: 1–17. https://doi.org/10.1186/s12866-022-02658-z.

Afriani, Arnim, Y. Marlida, and Yuherman, 2018. Isolation and characterization of lactic acid bacteria proteases from Bekasam for use as a beef tenderizer. Pakistan J Nutr. 17: 361–367. https://doi.org/10.3923/pjn.2018.361.367.

Angela, M. C., P. Di Ciccio, I. Ferrocino,T. Civera, F. T. Cannizzo and A. Dalmasso, 2023. Evaluation of the biofilm-forming ability and molecular characterization of dairy *Bacillus* spp. Isolates. Front. Cell. Infect. Microbiol., 13, https://doi.org/10.3389/fcimb.2023.1229460

Arulmani, M., K. Aparanjini, K. Vasanthi, P. Arumugam, M. Arivuchelvi, and P.T. Kalaichelvan, 2007. Purification and partial characterization of serine protease from thermostable alkalophilic *Bacillus laterosporus*-AK1. World J Microbiol Biotechnol. 23: 475–481. https://doi.org/10.1007/s11274-006-9249-7.

Bazaraa, W.A., A.A. Khattab, and E.M. Ibrahim, 2021. Mutagenesis and Protoplast Fusion for Enhanced Bacteriocins Production. Appl Food Biotechnol. 8: 133–142. https://doi.org/10.22037/afb.v8i2.32505.

Bhavani, B., B. Naveena, and N. Partha, 2012. Strain improvement of *streptomyces venezuelae* for enhanced fibrinolytic enzyme production. Adv Mater Res. 584: 440–444. https://doi.org/10.4028/www.scientific.net/AMR.584.440.

Bhosale, S., R. J. Desale and Y. G. Fulpagare, 2020. Biofilm: An Overview with Respect to Dairy Industry Int. J. Curr. Microbiol. App. Sci., 9: 150-156. https://doi.org/10.20546/ijcmas.2020.910.020.

Chaignon, P., I. Sadovskaya, C. Ragunah, N. Ramasubbu, J.B. Kaplan, and S. Jabbouri, 2007. Susceptibility of staphylococcal biofilms to enzymatic treatments depends on their chemical composition. Appl Microbiol Biotechnol. 75: 125–132. https://doi.org/10.1007/s00253-006-0790-y.

Chakraborty, U., and S.R. Sikdar, 2008. Production and characterization of somatic hybrids raised through protoplast fusion between edible mushroom strains *Volvariella volvacea* and *Pleurotus florida*. World J Microbiol Biotechnol. 24: 1481–1492. https://doi.org/10.1007/s11274-007-9630-1.

Chen, K.J., and C.K. Lee, 2018. Twofold enhanced dispersin B activity by N-terminal fusion to silver-binding peptide for biofilm eradication. Int J Biol Macromol. 118: 419–426. https://doi.org/10.1016/j.ijbiomac.2018.06.066.

Cortés, M.E., J.C. Bonilla, and R.D. Sinisterra, 2011. Biofilm formation, control and novel strategies for eradication. In: Science against microbial pathogens: communicating current research and technological advances. Méndez-Vilas A. (Ed.). FORMATEX: Spain. pages 896–905.

Dalmaso, G.Z.L., C.A.S. Lage, A.M. Mazotto., Dias E.P. de S., L.A. Caldas, D. Ferreira, and A.B. Vermelho, 2015. Extracellular peptidases from *Deinococcus radiodurans*. Extremophiles. 19: 989–999. https://doi.org/10.1007/s00792-015-0773-y.

Danson, M.J., D.T. Hough, R.J.M. Russell, G.L. Taylor, and L. Pearl, 1996. Enzyme thermostability and thermoactivity. Protein Eng Des Sel. 9: 629–630. https://doi.org/10.1093/protein/9.8.629.

Darwesh, O.M., A.S. El-Hawary, U.S. Kelany, and G.M. El-Sherbiny, 2019. Nematicidal activity of thermostable alkaline protease produced by *Saccharomonospora viridis* strain Hw G550. *Biotechnol Reports*. 24. https://doi.org/10.1016/j.btre.2019.e00386.

Darwesh, O.M., I.A. Elsehemy, M.H. El-Sayed, A.A. El-Ghamry, and A.S. El-Hawary, 2020. *Thermoflavimicrobium dichotomicum* as a novel thermoalkaliphile for production of environmental and industrial enzymes. Biointerface Res Appl Chem., 10: 4811–4820. https://doi.org/10.33263/BRIAC101.811820.

David, A., C. P. Singh, A. Kumar, S. Angural, D. Kumar, N. Puri, and N. Gupta, 2018. Coproduction of protease and mannanase from *Bacillus nealsonii* PN-11 in solid state fermentation and their combined application as detergent additives. Int J Biol Macromol., 108: 1176–1184. https://doi.org/10.1016/j.ijbiomac.2017.09.037.

Dwivedi, S., R. Wahab, F. Khan, Y.K. Mishra, J. Musarrat, and A.A. Al-Khedhairy, 2014. Reactive oxygen species mediated bacterial biofilm inhibition via zinc oxide nanoparticles and their statistical determination. PLoS One. 9: 1–9. https://doi.org/10.1371/journal.pone.0111289.

El-fadly, G.A.B., A.A.M. Abou-shoshah, and M.R.A. Rehan, 2009. Interspecific Streptomyces Protoplast Fusants as Biological Control Agents. Int J Environ Sci., 4: 37–44.

El-Hawary, A.S., 2015. Microbiological and Molecular Studies on some extremophilic Actinomycetes, MSc Thesis, Faculty of Science, Al-Azhar University, Cairo, Egypt.

El-Hawary, A.S., 2018. Microbiological and Biochemical Studies on Extremozymes produced by Actinomycetes and their Parasitological Applications, PhD dissertation, Faculty of Science, Al-Azhar University, Cairo, Egypt.

El-sayed, G.M., N.A. Abosereih, S.A. Ibrahim, A. Razik, B. Ashraf, M.A. Hammad, and F.M. Hafez, 2019. Cloning of the Organophosphorus Hydrolase (oph) Gene and Enhancement of Chlorpyrifos Degradation in the Achromobacter xylosoxidans Strain GH9OP via Mutation Induction Ghada. Jordan J Biol Sci. 12: 307–315.

El-Sherbini, A., and A.A. Khattab, 2018. Induction of novel mutants of *Streptomyces lincolnensis* with high lincomycin production. J Appl Pharm Sci., 8: 128–135. https://doi.org/10.7324/JAPS.2018.8220.

El-sherbiny, G.M., O.M. Darwesh, and A.S. El-hawary, 2017. Screening for Alkaline Proteases Produced by Thermophilic Actinomycetes Isolated from Egyptian Localities. Al Azhar Bull Sci. 9: 289–299.

Fleming D., and K. Rumbaugh, 2017. Approaches to Dispersing Medical Biofilms. Microorganisms. 5: 15. https://doi.org/10.3390/microorganisms5020015.

Folin O., and V. Ciocalteau, 1927. On tyrosine and tryptophan determinations in proteins. J Biol Chem., 73: 627–648.

Freese E.B., 1961. Transitions and transversions induced by depurinating agents. Proc Natl Acad Sci. 47: 540–545. https://doi.org/10.1073/pnas.47.4.540.

Friedlander, A., S. Nir, M. Reches and M. Shemesh, 2019. Preventing Biofilm Formation by Dairy-Associated Bacteria Using Peptide-Coated Surfaces. Front. Microbiol. 10:1405. doi: 10.3389/fmicb.2019.01405.

Fujii T., K. Fukano, K. Hirano, A. Mimura, M. Terauchi, S.I. Etoh, and A. Iida, 2020. A new serine protease family with elastase activity is produced by *Streptomyces* bacteria. Microbiology. 166: 253–261. https://doi.org/10.1099/mic.0.000880.

Fulaz S., S. Vitale, L. Quinn, *et al*., 2019. Nanoparticl-biofilm interactions: the role of the EPS matrix. Trends Microbiol., 27: 915–26. https://doi.org/10.1016/j.tim.2019.07.004

Geng C., X. Nie, Z. Tang, Y. Zhang, J. Lin, M. Sun, and D. Peng, 2016. A novel serine protease, Sep1, from *Bacillus firmus* DS-1 has nematicidal activity and degrades multiple intestinal-associated nematode proteins. Sci Rep. 6: 1–12. https://doi.org/10.1038/srep25012.

Godson G.N., and Vapnek D. (1973). A simple method of preparing large amounts of ΦX174 RF I supercoiled DNA. BBA Sect Nucleic Acids Protein Synth. 299: 516–520. https://doi.org/10.1016/0005-2787(73)90223-2.

Hopwood D.A., M.J. Bibb, K.F. Chater, T. Kieser, C.J. Bruton, H.M. Kieser, *et al*., 1985. Genetic manipulation of *Streptomyces*: A laboratory manua. The John Innes Foundation: Norwich (UK).

Ibrahim A.S.S., A.A. Al-Salamah, Y.B. El-Badawi, M.A. El-Tayeb, and G. Antranikian, 2015. Detergent-, solvent- and salt-compatible thermoactive alkaline serine protease from halotolerant alkaliphilic *Bacillus* sp. NPST-AK15: purification and characterization. Extremophiles. 19: 961–971. https://doi.org/10.1007/s00792-015-0771-0.

Jee S.C., M. Kim, J.S. Sung, and A.A. Kadam, 2020. Efficient biofilms eradication by enzymatic-cocktail of pancreatic protease type-i and bacterial α-amylase. Polymers (Basel). 12: 1–13. https://doi.org/10.3390/polym12123032.

Kamran A., H. Ur Rehman, S.A. Ul Qader, A.H. Baloch, and M. Kamal, 2015. Purification and characterization of thiol dependent, oxidation-stable serine alkaline protease from thermophilic *Bacillus* sp. J Genet Eng Biotechnol. 13: 59–64. https://doi.org/10.1016/j.jgeb.2015.01.002.

Khan M.A., N. Ahmad, A.U. Zafar, and I.A. Nasir, 2011. Isolation and screening of alkaline protease producing bacteria and physio-chemical characterization of the enzyme. Afr J Biotechnol., https://doi.org/10.5897/AJB11.413.

Khattab A.A., and M.S. Abdel-Aziz, 2012. Mutation induction and protoplast fusion of *Streptomyces* spp. For enhanced alkaline protease production. J Appl Sci Res. 8: 807–814.

Kim L.H., S.J. Kim, C.M. Kim, M.S. Shin, S. Kook, and I.S. Kim, 2013. Effects of enzymatic treatment on the reduction of extracellular polymeric substances (EPS) from biofouled membranes. Desalin Water Treat. 51: 6355–6361. https://doi.org/10.1080/19443994.2013.780996.

Kumar S.S., M. Haridas, and A. Sabu, 2018. Process optimization for production of a fibrinolytic enzyme from newly isolated marine bacterium *Pseudomonas aeruginosa* KU1. Biocatal Agric Biotechnol., 14: 33–39. https://doi.org/10.1016/j.bcab.2018.02.001.

Laemmli U.K., 1970. Cleavage of structural proteins during the assembly of the head of bacteriophage T4. Nature, 227: 680–685. https://doi.org/10.1038/227680a0.

Lakshmi B.K.M., D. Muni Kumar, and K.P.J. Hemalatha, 2018. Purification and characterization of alkaline protease with novel properties from *Bacillus cereus* strain S8. J Genet Eng Biotechnol., 16: 295–304. https://doi.org/10.1016/j.jgeb.2018.05.009.

Lequette Y., G. Boels, M. Clarisse, and C. Faille, 2010. Using enzymes to remove biofilms of bacterial isolates sampled in the food-industry. Biofouling. 26: 421–431. https://doi.org/10.1080/08927011003699535.

Liaqat I., T. Hussain, A.W. Qurashi, G. Saleem, A. Bibi, M.F. Qamar, *et al*., 2021. Antibiofilm activity of proteolytic enzymes against *salmonella gallinarum* isolates from commercial broiler chickens. Pak J Zool. 53: 1111–1118. https://doi.org/10.17582/JOURNAL.PJZ/20191029131040.

Lowry, O. H., N. J. Rosebrough, A. L. Farr and R. J. Randall, (1951). Protein measurement with the Folin phenol reagent. Journal of Biological Chemistry. 193 (1): 265–75. doi:10.1016/S0021-9258(19)52451-6

Lu J., C. Guo, J. Li, H. Zhang, G. Lu, Z. Dang, and R. Wu, 2013. A fusant of *Sphingomonas* sp. GY2B and *Pseudomonas* sp. GP3A with high capacity of degrading phenanthrene. World J Microbiol Biotechnol., 29: 1685–1694. https://doi.org/10.1007/s11274-013-1331-3.

Madan M., S. Dhillon, and R. Singh, 2002. Purification and characterization of alkaline protease from a mutant of *Bacillus polymyxa*. Indian J Microbiol. 42: 155–159. https://doi.org/10.5829/idosi.abr.2015.9.1.91112.

Maeda T., T. Yoshimura, R. García-contreras, and H.I. Ogawa, 2011. Purification and characterization of a serine protease secreted by *Brevibacillus* sp. KH3 for reducing waste activated sludge and biofilm formation. Bioresour Technol. 102: 10650–10656. https://doi.org/10.1016/j.biortech.2011.08.098.

Mahmoud A., E. Kotb, A.I. Alqosaibi, A.A. Al-Karmalawy, I.S. Al-Dhuayan, and H. Alabkari, 2021. In vitro and in silico characterization of alkaline serine protease from *Bacillus subtilis* D9 recovered from Saudi Arabia. Heliyon. 7. https://doi.org/10.1016/j.heliyon.2021.e08148.

Marchand S., Block J. De, Jonghe V. De, A. Coorevits, M. Heyndrickx, and L. Herman (2012). Biofilm Formation in Milk Production and Processing Environments; Influence on Milk Quality and Safety. Compr Rev Food Sci Food Saf. 11: 133–147. https://doi.org/10.1111/j.1541-4337.2011.00183.x.

Mechri S., M. Kriaa, Elhoul Berrouina M. Ben, M. Omrane Benmrad, N. Zaraî Jaouadi and H. Rekik, *et al*. (2017). Optimized production and characterization of a detergent-stable protease from *Lysinibacillus fusiformis* C250R. Int J Biol Macromol. 101: 383–397. https://doi.org/10.1016/j.ijbiomac.2017.03.051.

Mehdi W.A., A.A. Mehde, M. Özacar, and Z. Özacar, 2018. Characterization and immobilization of protease and lipase on chitin-starch material as a novel matrix. Int J Biol Macromol., 117: 947–958. https://doi.org/10.1016/j.ijbiomac.2018.04.195.

Mehtani P., C. Sharma, and P. Bhatnagar, 2017. Strain Improvement of *Halotelerant Actinomycete* for Protease Production by Sequential Mutagenesis. Int J Chem Sci., 15: 109–115.

Meireles A., Borges A., Giaouris E., and Simões M. (2016). The current knowledge on the application of anti-biofilm enzymes in the food industry. *Food Res Int., 86: 140–146.* https://doi.org/10.1016/j.foodres.2016.06.006.

Mitrofanova O., A. Mardanova, V. Evtugyn, L. Bogomolnaya, and M. Sharipova, 2017. Effects of *Bacillus* Serine Proteases on the Bacterial Biofilms. Biomed Res Int., 2017: 1-11. https://doi.org/10.1155/2017/8525912.

Mohd Yusof H., R. Mohamad, U.H. Zaidan, *et al*. 2020. Sustainable microbial cell nanofactory forzinc oxide nanoparticles production by zinc-tolerant probiotic *Lactobacillus plantarum* strain TA4. Microbial cell factories 19: 1–7. https://doi.org/10.1186/s12934-020-1279-6

Okanishi M., K. Suzuki, and H. Umezawa, 1974. Formation and Reversion of *Streptomycete* Protoplasts : Cultural Condition and Morphological Study. J Gen Microbiol., 80: 389–400. https://doi.org/https://doi.org/10.1099/00221287-80-2-389.

Padmapriya B., T. Rajeswari, R. Nandita, and F. Raj, 2012. Production and purification of alkaline serine protease from marine *Bacillus* species and its application in detergent industry. Eur J Appl Sci., 4: 21–26.

Park J.H., J.H. Lee, M.H. Cho, M. Herzberg, and J. Lee, 2012b. Acceleration of protease effect on Staphylococcus aureus biofilm dispersal. FEMS Microbiol Lett. 335: 31–38. https://doi.org/10.1111/j.1574-6968.2012.02635.x.

Park J.H., J.H. Lee, C.J. Kim, J.C. Lee, M.H. Cho, and J. Lee, 2012a. Extracellular protease in Actinomycetes culture supernatants inhibits and detaches Staphylococcus aureus biofilm formation. Biotechnol Lett., 34: 655–661. https://doi.org/10.1007/s10529-011-0825-z.

Patil A M.R. (2014). Role of Extracellular Proteases in Biofilm Disruption of Gram Positive Bacteria with Special Emphasis on *Staphylococcus aureus* Biofilms. Enzym Eng. 04: 1–7. https://doi.org/10.4172/2329-6674.1000126.

Prabavathy V.R., N. Mathivanan, E. Sagadevan, K. Murugesan, and D. Lalithakumari, 2006. Intra-strain protoplast fusion enhances carboxymethyl cellulase activity in *Trichoderma reesei*. Enzyme Microb Technol. 38: 719–723. https://doi.org/10.1016/j.enzmictec.2005.11.022

Pratika M., M. Ananda and I. N. Suwastika, 2021. Protease activity from bacterial isolates of *Nepenthes maxima* reinw. Ex nees. Journal of Physics: Conference Series. DOI 10.1088/1742-6596/1763/1/012092.

Qi H.Y., and Y.X. Zheng, 1990. Interspecific protoplast fusion in Streptomyces--selection of thermotolerant antibiotic-producing recombinant. Chin J Biotechnol. 6: 139–147.

Radwan A.A., O.M. Darwesh, M.T. Emam, K.A. Mohamed, and H.M. Abu Shady, 2022. A combined treatment of Proteinase K and biosynthesized ZnO-NPs for eradication of dairy biofilm of sporeformers. AIMS Microbiol. 8: 507–527. https://doi.org/10.3934/microbiol.2022033.

Raissa G., D.E. Waturangi, and D. Wahjuningrum, 2020. Screening of antibiofilm and anti-quorum sensing activty of Actinomycetes isolates extracts against aquaculture pathogenic bacteria. BMC Microbiol. 20: 1–10. https://doi.org/10.1186/s12866-020-02022-z.

Ramkumar A., N. Sivakumar, A.M. Gujarathi, and R. Victor, 2018. Production of thermotolerant, detergent stable alkaline protease using the gut waste of *Sardinella longiceps* as a substrate: Optimization and characterization. Sci Rep. 8: 1–15. https://doi.org/10.1038/s41598-018-30155-9.

Sadiq F.A., S. Flint, L. Yuan, Y. Li, T.J. Liu, and G.Q. He, 2017. Propensity for biofilm formation by aerobic mesophilic and thermophilic spore forming bacteria isolated from Chinese milk powders. Int J Food Microbiol. 262: 89–98. https://doi.org/10.1016/j.ijfoodmicro.2017.09.015.

Sambrook J., and Russell D.W. (2001). Molecular Cloning, a laboratory manual. 3rd edition, *Cold Spring Harbor Laboratory Press*, Cold Spring Harbor: New York.

Sarkar G., and K. Suthindhiran, 2020. Isolation and Bioprocess Optimization of Halophilic and Alkaline Protease from Marine Streptomyces and Its Use as Contact Lens Cleaner. Research Square. 1–25.

Sharma S.G., A. Walia, A. Chauhan, and C.K. Shirkot, 2021. Statistical optimization of alkaline protease from *Bacillus amyloliquefaciens* SP1. Indian J Exp Biol., 59: 421–432.

Shemesh M., and Ostrov I. (2020). Role of *Bacillus* species in biofilm persistence and emerging antibiofilm strategies in the dairy industry. J Sci Food Agric., 100: 2327–2336. https://doi.org/10.1002/jsfa.10285.

Shkodenko L, I. Kassirov, E. Koshel, 2020. Metal oxide nanoparticles against bacterial biofilms: perspectives and limitations. Microorganisms 8: 1–21. https://doi.org/10.3390/microorganisms8101545.

Smolin D., N. Tötsch, J.N. Grad, J. Linders, F. Kaschani, M. Kaiser, *et al*., 2020. Accelerated trypsin autolysis by affinity polymer templates. RSC Adv. 10: 28711–28719. https://doi.org/10.1039/d0ra05827k.

Sumardi, Agustrina R., C.N. Ekowati, and Y.S. Pasaribu, 2018. Characterization of protease from *bacillus* sp. on medium containing $FeCl_3$ exposed to magnetic field 0.2 mt. IOP Conf Ser Earth Environ Sci., 130: 0–12. https://doi.org/10.1088/1755-1315/130/1/012046.

Verma N., M.C. Bansal, and V. Kumar, 2008. Protoplast fusion technology and its biotechnological applications. Chem Eng Trans.14:113-20.

Yang S., Y. Wang, F. Ren, Z. Li, Q. Dong, 2023. Applying enzyme treatments in Bacillus cereus biofilm removal, LWT - Food Science and Technology 180. https://doi.org/10.1016/j.lwt.2023.114667.

Yasumitsu H., 2017. Serine protease zymography: Low-cost, rapid, and highly sensitive RAMA casein zymography. In: Methods in Molecular Biology. Humana Press: New York. pages 13–24. https://doi.org/10.1007/978-1-4939-7111-4_2.

Yeoman K.H., and C. Edwards, 1994. Protease production by *Streptomyces thermovulgaris* grown on rapemeal-derived media. Journal of Applied Bacteriology. 77: 264–270.

Zhang X.X., H.Y. Jia, B. Wu, D.Y. Zhao, W.X. Li, and S.P. Cheng, 2009. Genetic analysis of protoplast fusant Xhhh constructed for pharmaceutical wastewater treatment. Bioresour Technol. 100: 1910–1914. https://doi.org/10.1016/j.biortech.2008.10.012.

Zhou X.F., and Zhou Q. (1989). Interspecific protoplast fusion of *Streptomyces hygroscopicus* var. *yingchengenisis* with *Streptomyces qingfengmyceticus* and biological characterization of their recombinants. Chin J Biotechnol., 5: 161–166.